



INSTITUT DE FRANCE  
Académie des sciences

# *Comptes Rendus*

---

## *Physique*

Tanguy Rouxel

**Some strange things about the mechanical properties of glass**

Volume 24, Special Issue S1 (2023), p. 99-112


Online since: 18 January 2023

Issue date: 26 April 2024

**Part of Special Issue:** From everyday glass to disordered solids

**Guest editors:** Jean-Louis Barrat (Université Grenoble-Alpes, France) and Daniel Neuville (Université de Paris, Institut de physique du globe de Paris, CNRS, France)

<https://doi.org/10.5802/crphys.126>

 This article is licensed under the  
CREATIVE COMMONS ATTRIBUTION 4.0 INTERNATIONAL LICENSE.  
<http://creativecommons.org/licenses/by/4.0/>



*The Comptes Rendus. Physique are a member of the  
Mersenne Center for open scientific publishing*  
[www.centre-mersenne.org](http://www.centre-mersenne.org) — e-ISSN : 1878-1535



---

From everyday glass to disordered solids / *Du verre quotidien aux solides désordonnés*

## Some strange things about the mechanical properties of glass

*Quelques étrangetés sur les propriétés mécaniques du verre*

Tanguy Rouxel<sup>✉, a, b</sup>

<sup>a</sup> Glasses and Mechanics Lab., Physics Institute (IPR), UMR UR1-CNRS 6251, Université de Rennes, Campus de Beaulieu, 35042 Rennes cedex, France

<sup>b</sup> Institut Universitaire de France, France

E-mail: [tanguy.rouxel@univ-rennes1.fr](mailto:tanguy.rouxel@univ-rennes1.fr)

**Abstract.** Glasses and crystals from the same chemical system mostly share the same interatomic bond strength. Nevertheless, they differ by the arrangement of bonds in space, which gives birth to different atomic packing efficiencies. We show in this review that as far as the elastic moduli and hardness are concerned, the atomic packing density predominates over the bond strength. The shear modulus of crystalline phases is usually much larger than the one of glasses with the same stoichiometric composition, thanks to a more efficient packing of atoms in the former. In contrast, the increase in hardness is quite limited, likely because of the additional contribution of dislocation activity to the deformation processes beneath the indenter in the case of crystals (shear plasticity). We also show that the occurrence of chemical heterogeneities (weak channels) at the mesoscopic scale in glasses, which is often associated with the lack of long range atomic ordering, promotes easy fracture paths and is responsible for the low toughness and fracture surface energy.

**Résumé.** Les verres et les cristaux issus du même système chimique partagent généralement la même force de liaison interatomique. Néanmoins, ils diffèrent par l'arrangement des liaisons dans l'espace, ce qui donne lieu à des efficacités d'empaquetage atomique différentes. Nous montrons dans cette étude qu'en ce qui concerne les modules élastiques et la dureté, la densité d'empilement atomique prédomine sur la force de liaison. Le module de cisaillement des phases cristallines est généralement beaucoup plus élevé que celui des verres ayant la même composition stœchiométrique, grâce à un empilement plus efficace des atomes dans les premières. En revanche, l'augmentation de la dureté est assez limitée, probablement en raison de la contribution supplémentaire de l'activité des dislocations aux processus de déformation sous l'indenteur dans le cas des cristaux (plasticité de cisaillement). Nous montrons également que l'apparition d'hétérogénéités chimiques (canaux faibles) à l'échelle mésoscopique dans les verres, qui est souvent associée à l'absence d'ordonnement atomique à longue portée, favorise les chemins de rupture facile et est responsable de la faible ténacité et de la faible énergie de surface de rupture.

*Manuscript received 17 June 2022, revised 21 September 2022, accepted 5 October 2022.*

## 1. Introduction

There are some general trends in materials science regarding the mechanical properties. For example, the elastic moduli mostly correlate with the melting point [1], and ductility usually comes with softness [2]. As a matter of fact, ductile metals such as copper, lead, silver or aluminum are softer than beryllium, titanium, tungsten or chromium, which behave in a more brittle manner. Besides, as materials become stronger, they often become more brittle. The gain in strength in high carbon steel comes at the expense of ductility. Ceramics are strong, but brittle. Polymers are soft and easy to shape.

Nevertheless, a look at the fine details of the changes of the properties with composition, shows that the intuitive tendencies are not always followed and that the physics behind the mechanical behavior is mostly incompletely taken into account. Glasses offer a unique opportunity to follow the property change in a very smooth way, and across chemical systems where the interatomic bonding character evolves from metallic, to ionic and covalent. A review and a comparative analysis of the mechanical properties of glasses, including elasticity, hardness, strength, toughness and viscosity, across metallic, chalcogenide, silicate, oxynitride and oxycarbide glass forming chemical systems bring to light some striking features. Just to mention a few of them: (1) the stiffest glasses, that is those with the largest elastic moduli, are not those with the strongest interatomic bonds; (2) glasses are mostly much less rigid but nearly as hard as their crystalline polymorphs (same stoichiometry), and the softest (less hard) glasses are also the most brittle ones; (3) despite the fact that glasses break in an ideally brittle manner, with almost no visible permanent deformation at fracture and adopt an elastic behavior at temperatures below their glass transition temperature (say  $T < 0.5T_g$ ), they can be indented and scratched, so that some permanent deformation mechanism shows up below  $T_g$ , where viscous flow can be neglected; (4) although inorganic glasses are brittle and their elastic moduli are exceeded by those of numerous metals, their intrinsic (or ultimate) strength is exceptional and reach the values proposed for the theoretical strength of materials; and (5) there are “fragile” liquids (per Angell concept) that turn out to result in tough glasses!

Each chemical system brings some pieces to the puzzle of the global picture. For instance, compositional effects within silicate glasses shed light on the key role of the atomic packing density, and those within chalcogenide glasses reflect the importance of the average atomic network cross-linking, while metallic glasses (MGs), in comparison with oxide and chalcogenide ones, show what is going on when the interatomic bonds are losing their directionality and their topological constraints.

## 2. The elastic moduli and Poisson’s ratio of glasses

The elastic moduli of metals, and especially the shear modulus, were often reported to be correlated to the melting point, that is to the dissociation energy ( $\langle U_0 \rangle$ ). However, an elastic modulus is given in pascals, that is in  $\text{J}\cdot\text{m}^{-3}$ , whereas the dissociation energy is expressed in  $\text{J}\cdot\text{mol}^{-1}$ . Elastic moduli, and in the first place the bulk modulus ( $K$ ), are governed by the distribution of bonds in space, and thus involve the atomic packing density ( $C_g$ ). For an arbitrary oxide glass composition  $\langle U_0 \rangle$  can be estimated from the dissociation enthalpy of each oxide ( $\text{A}_x\text{O}_y$ ) introduced in the composition [3, 4],  $\Delta H_d$ , which is given by a classical Born–Haber cycle:  $\Delta H_d = -\Delta H_f(\text{A}_x\text{O}_y) + x\Delta H_{\text{at}}(\text{A}) + y\Delta H_{\text{at}}(\text{O})$ , where  $\Delta H_f$  is an enthalpy of formation and  $\Delta H_{\text{at}}$  is an atomization enthalpy (see [4] for details):

$$\langle U_0 \rangle = \sum_i x_i \Delta H_{\text{di}} \quad (1)$$

where  $x_i$  and  $\Delta H_{di}$  are respectively the molar fraction and the dissociation enthalpy of the  $i$ th oxide contribution to the gram-atom of glass. In the case of a metallic glass,  $\langle U_0 \rangle$  was estimated from existing thermochemistry data [5, 6] for the elements constituting the studied glasses. For example, in the case of a binary system,

$$\langle U_0 \rangle = x\Delta H_{at}(A, g) + y\Delta H_{at}(B, g) - y\Delta H_{mixing}(A_xB_y) \quad (2)$$

where  $\langle U_0 \rangle$  represents the dissociation energy (standard pressure), i.e. the energy necessary to obtain separate gaseous atoms from the solid material (a gram-atom is considered:  $x + y = 1$ ). The enthalpy of mixing is rarely known for multiconstituent metallic liquids. Furthermore, it might not represent the situation in amorphous systems, inasmuch as the glassy network exhibits some peculiar structural features such as chemical segregation, clustering etc. Nevertheless, in most cases, it seems that the enthalpy of mixture is much smaller than the atomization enthalpy in absolute values. The atomisation (sublimation) enthalpy is typically of several hundreds  $\text{kJ}\cdot\text{mol}^{-1}$  (605, 326, 431, and 338 for Zr, Al, Ni and Cu respectively), whereas the enthalpy of mixing is less than the enthalpy of formation (about  $-34 \text{ kJ}\cdot\text{mol}^{-1}$  for ZrCu,  $-57 \text{ kJ}\cdot\text{mol}^{-1}$  for PdSi,  $-30 \text{ kJ}\cdot\text{mol}^{-1}$  for  $\text{Ni}_5\text{P}\dots$ ) and is of few tens  $\text{kJ}\cdot\text{mol}^{-1}$  [7]. In the case of a disordered arrangement of atoms,  $C_g$  can be determined from the ratio of the effective volume occupied by a mole of atoms ( $V_a$ ), as estimated from the atomic radii ( $V_a = \mathcal{N} \sum_i (4/3)\pi x_i r_i^3$ , where  $\mathcal{N}$  is Avogadro number,  $x_i$  and  $r_i$  are the atomic fraction and ionic radius of the  $i$ th element), to the corresponding volume of glass ( $V_0$ ), calculated from the specific mass of the glass ( $\rho$ ) and the molar mass of the constituents ( $V_0 = (1/\rho) \sum_i x_i m_i$ , where  $m_i$  is the molar mass of the  $i$ th element):

$$C_g = \frac{\mathcal{N} \sum_i (4/3)\pi x_i r_i^3}{(\sum_i x_i m_i) / \rho}. \quad (3)$$

In multiconstituent systems where atoms are relatively free to explore the empty space of the atomic network, large  $C_g$  values may be obtained. This situation is observed in MGs based on precious metals, which exhibit  $C_g$  values as large as 0.8. In the case of silicate glasses,  $C_g$  ranges typically between 0.45 and 0.55 [8–10]. Most metals crystallized in dense structures involving close-packed arrangements of atoms such as in the face-centered cubic and hexagonal compact lattices, which both correspond to a value of  $C_g$  of 0.74 (pure substances). This is why in the case of metals the elastic moduli are mainly correlated with the dissociation energy. The situation is very different in the case of glasses since the presence of free volume and of directional bonds (non-metallic systems) result in relatively loose-packed atomic arrangements for which  $C_g$  spreads over a wide interval, typically from 0.41 for silicon-oxycarbide glasses to 0.48 for precious metal based MGs. As a matter of fact, there is no one to one relationship between  $K$  and  $\langle U_0 \rangle$  (Figure 1). For example,  $K$  is around 114 GPa for  $\text{Pd}_{80}\text{Si}_{20}$  and  $\text{Zr}_{55}\text{Co}_{25}\text{Al}_{20}$  MGs and for a  $\text{Y}_{14.1}\text{Si}_{18.5}\text{Al}_{5.3}\text{O}_{54.7}\text{N}_{7.5}$  oxynitride glass (horizontal dashed straight line in Figure 1), although the values for  $\langle U_0 \rangle$  are respectively of 392.8, 504 and 641  $\text{kJ}\cdot\text{mol}^{-1}$ . In these glasses, the decrease of the atomic packing density counterbalances the increase in  $\langle U_0 \rangle$  (or in  $T_g$ ). The same observation can be made with Young's modulus. For example,  $\text{Tm}_{53}\text{Al}_{25}\text{Co}_{20}$ , amorphous silica (a-SiO<sub>2</sub>), a standard window glass (soda-lime-silica) and an electric glass (E-glass) (about 54 mol% Al<sub>2</sub>O<sub>3</sub>, 22 mol% B<sub>2</sub>O<sub>3</sub>, 14 mol% AE and 10 mol% A) have a common Young's modulus value close to 70 GPa, as for aluminum, despite the fact that their glass transition temperatures spread over the 277–1190 °C interval. Let us consider the case of vitreous silica. The bulk modulus ( $K$ ) of a-SiO<sub>2</sub> is equal to 33 GPa. The addition of 30 mol% of a mixture of alkaline (A) and alkaline-earth (AE) oxides (Na<sub>2</sub>O, K<sub>2</sub>O, MgO, CaO), to meet a standard composition for window glasses, leads to a value of 44 GPa for  $K$ , that is a larger value in spite of much smaller bond energies for the added constituents:  $U_{0(\text{Na-O})} = 73 \text{ kJ}\cdot\text{mol}^{-1}$ ,  $U_{0(\text{K-O})} = 49 \text{ kJ}\cdot\text{mol}^{-1}$ ,  $U_{0(\text{Mg-O})} = 166 \text{ kJ}\cdot\text{mol}^{-1}$ , and  $U_{0(\text{Ca-O})} = 177 \text{ kJ}\cdot\text{mol}^{-1}$ , whereas  $U_{0(\text{Si-O})} = 624 \text{ kJ}\cdot\text{mol}^{-1}$ . However,  $C_g$  is increased in the

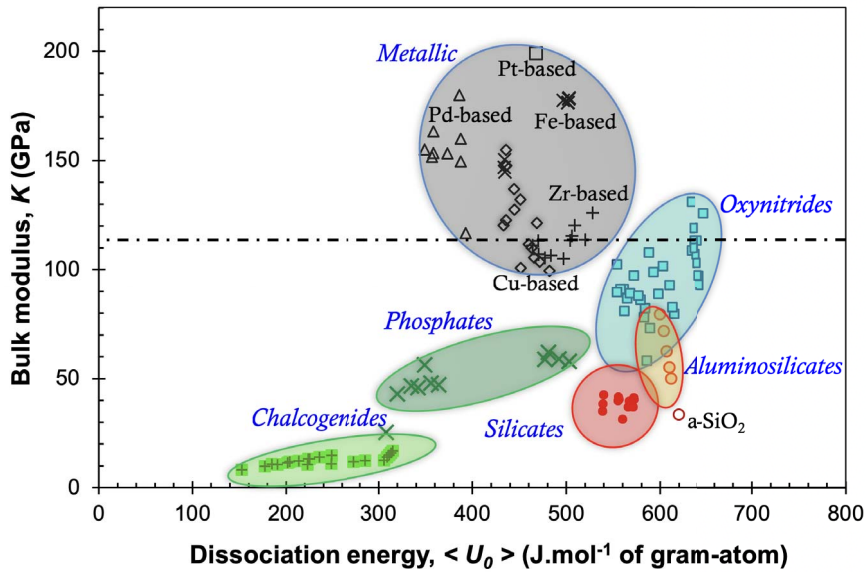


**Figure 1.** The bulk modulus of glasses from different chemical systems as a function of the dissociation energy per mole of gram-atom. Data were extracted from Refs. [4, 6]. The horizontal dashed line intersects with different glass compositions exhibiting the same  $K$  value.

presence of  $A$  and  $AE$  oxides, to about 0.516 for a standard window glass, while it is as small as 0.454 for  $a\text{-SiO}_2$ . This is another clear evidence for the role played by  $C_g$  on the elastic moduli which kills off the myth that strong bonds make stiff materials!

Let us move one step further in the interpretation of the dependence of the elastic moduli on the glass composition by looking at the correlation between  $K$  and the volume density of energy,  $\langle U_0 \rangle / \langle V_0 \rangle$  (Figure 2). It turns out that for a given chemical system, the data points are quite nicely aligned. Nevertheless, the rates at which  $K$  changes with the volume density of energy differ from one series to the other. The slope is relatively steep for metallic glasses. It reaches about 3.6 for those with palladium or platinum as the major host elements, it is smaller for Zr-, Cu-, and Ti-based alloys (about 2.5) and is at about 1.5 for rare-earth-based ones. In the case of phosphate glasses,  $K \approx \langle U_0 \rangle / \langle V_0 \rangle$ . The slope is equal to 3/4 in average for silicates and tends to increase with nitrogen in silicon-oxynitride glasses. Actually, the rate at which  $K$  changes with  $\langle U_0 \rangle / \langle V_0 \rangle$  reflects the interatomic bonding character. For sake of simplicity, considering a Lennard–Jones (L–J) type potential for the driving force of elasticity at the atomic or structural network scale, with  $m$  and  $n$  being the exponents associated with the repulsive and attractive branches of the potential, then  $K / (\langle U_0 \rangle / \langle V_0 \rangle)$  is proportional to the  $mn$  product (this is known as the 1st Grüneisen’s rule). Despite some fundamental difficulties, including (i) the transposition of the approach to the dissociation energy  $\langle U_0 \rangle$ , which is not an interatomic bond strength, and (ii) the assumption that the cohesive energy can be differentiated with respect to the atomic volume (see Ref. [6] for details), the present investigations suggest a steep potential for MGs and especially those based on precious metals, which leaves little room for changes in the inter-unit distance, so that shear is expected to predominate, in agreement with the fact that Poisson’s ratio ( $\nu$ ) is relatively large for these glasses. Here, a structural unit can be either an atom, a group of atoms representative of the glass stoichiometry, or a cluster with a peculiar chemical composition, depending on the way the glass behaves under mechanical loading at the atomic scale, as illustrated in the

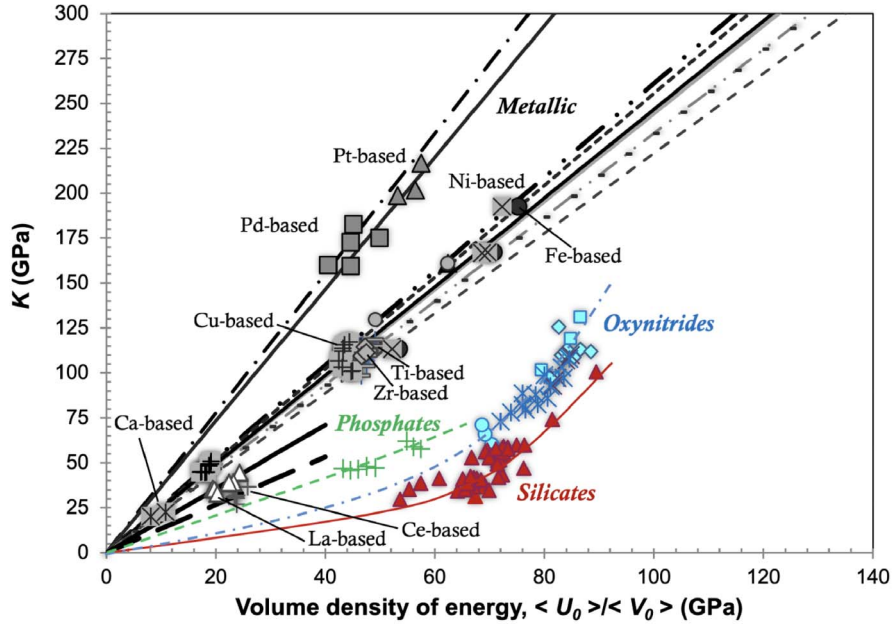


**Figure 2.** The bulk modulus of glasses from different chemical systems as a function of the volume density of energy (in  $\text{J}\cdot\text{m}^{-3}$  or in GPa). Marks correspond to different chemical systems. Data were extracted from Refs. [4, 6].

schematic drawings at the bottom in Figure 3. On the contrary, for a relatively small  $mn$  product, the structural units might move each with respect to the others with center-to-center distance variations and local volume contraction or expansion. In the case of precious-metal (Pt, Au, Pd, ...) based MGs, the atomic packing efficiency reaches 0.8, and  $\nu$  meets values as large as 0.4. In the case of oxide glasses, it is noteworthy that whatever the chemical system,  $\nu$  and  $C_g$  are significantly smaller than for the MGs, and so is the  $mn$  product. For silicate glasses,  $C_g$  is typically between 0.4 and 0.55, and  $K/(\langle U_0 \rangle / \langle V_0 \rangle) < 1$ , consistently with the fact that oxide glasses are much more brittle than the metallic ones, and undergo significant “permanent” volume changes under mechanical loading (for instance pure  $\text{SiO}_2$  glass, with  $\nu \approx 0.15$ , can experience up to 20% densification under hydrostatic loading) [11]. The explanation chiefly lies in the atomic packing density, which mostly gets better and better as the network cross-linking degree and the bond strength are decreased. As a matter of fact, it is easier to pack “hard” spheres, such as “good” metal atoms, in a box, than stiff structural units such as rods, triangles or even worse, tetrahedra!

### 3. Hardness and permanent deformation mechanism at an indentation site

Typical hardness ( $H$ ) values for inorganic, non-metallic glasses range between 1 (chalcogenides) and 12 (silicon-oxynitrides) GPa [12]. It is noteworthy that the apparent hardness, as measured by means of indentation methods, is known to change with the applied load ( $P$ )—a decrease of  $H$  is mostly observed with an increase of  $P$ —, with the loading rate and duration, and with the environment. For  $\alpha\text{-SiO}_2$ ,  $H$  decreases from  $\approx 11.3$  to  $\approx 6.3$  GPa as the load increases from 10 mN to 1 N, and for a standard window glass it changes from  $\approx 6.3$  to 4.5 GPa as the load increases from 10 mN to 10 N; this is the so-called Indentation-Size-Effect (ISE) [13–15]. Besides,  $H$  depends on the way the glass is processed, and the purity of the constituents. As a matter of fact, different values are reported for vitreous silica. For example, in the case of

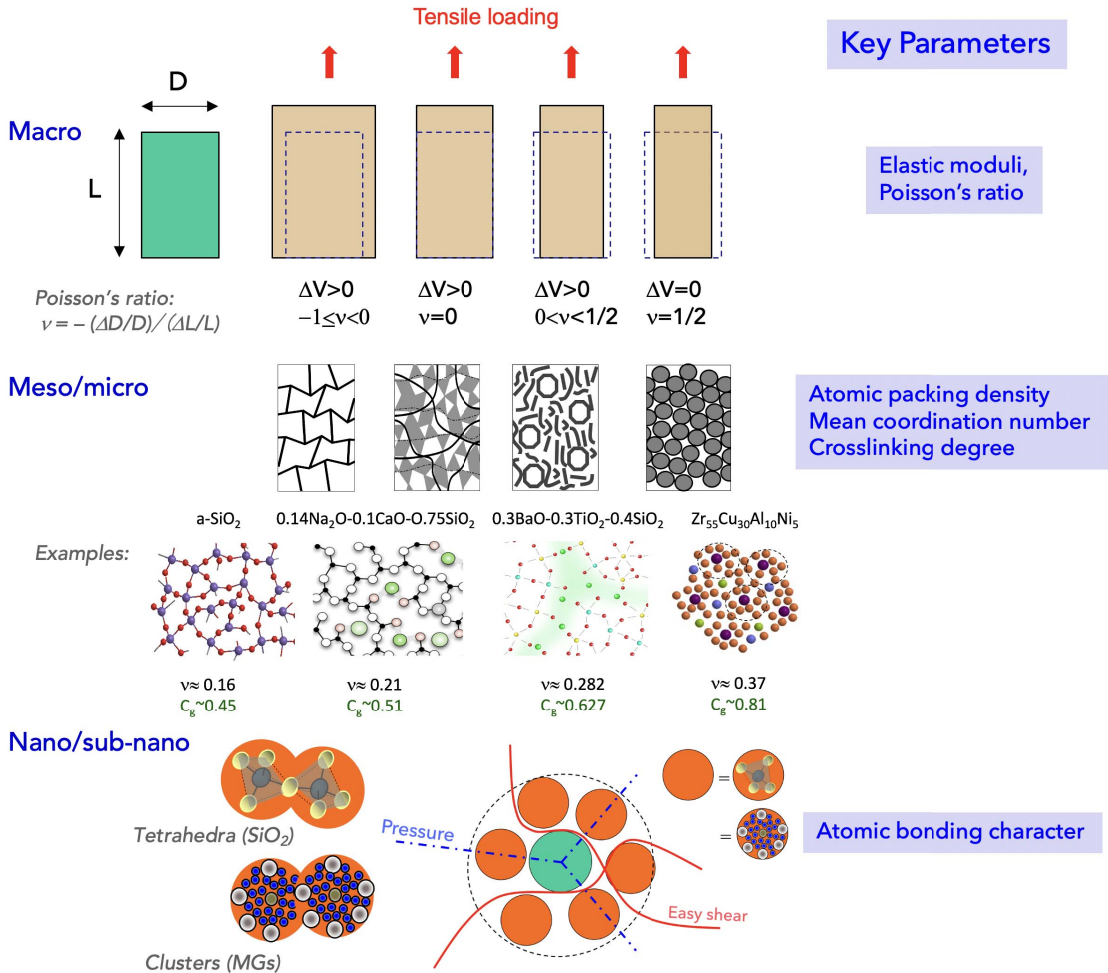


**Figure 3.** Schematic drawings of the way Poisson's ratio, a macroscopic elastic property, correlates to the fine details of the deformation kinematics.

fused silica glasses, hardness as obtained by means of a Vickers indentation test at 1 N for 15 s is 8.7 GPa for a “vitreosil” glass (Saint-Gobain Co.) [15], whereas in the same conditions,  $H = 9.6$  GPa for a “suprasil” (Heraeus Conamic Co.) [16]. Hardness was found to scale with  $\mu$  in many crystallized systems and is also more or less scaling with the melting point,  $T_m$ , for crystals and with  $T_g$  for glasses. But these are rough approximations (Figure 4) since, on the one hand, the atomic packing factor is ignored, on the other different mechanisms may result in the same hardness number. For example, the dashed line in Figure 4 crosses data points associated with a hardness of 7 GPa and corresponding to glass compositions from very different systems, including  $\text{Cu}_{60}\text{Hf}_{10}\text{Zr}_{20}\text{Ti}_{10}$  ( $T_g = 481$  °C),  $\text{Si}_{0.168}\text{Ca}_{0.084}\text{Mg}_{0.084}\text{Al}_{0.064}\text{O}_{0.6}$  ( $T_g = 732$  °C) and  $a\text{-SiO}_2$  ( $T_g = 1190$  °C).  $\text{As}_{0.2}\text{Se}_{0.8}$ ,  $\text{B}_{0.08}\text{Ca}_{0.09}\text{P}_{0.18}\text{O}_{0.65}$ , and  $\text{Ce}_{70}\text{Al}_{10}\text{Ni}_{10}\text{Cu}_{10}$  glasses have also the same hardness,  $H = 1.5$  GPa, despite very different transition temperatures (from 97 °C for the chalcogenide composition to 611 °C for the boro-phosphate one). The hardness of glasses containing a large free volume content, such as vitreous silica ( $a\text{-SiO}_2$ ), is predominantly controlled by the volume density of atomic bonds, regardless of the interatomic bond energy. This is the reason behind  $a\text{-SiO}_2$  ( $H \approx 7\text{--}9$  GPa) being softer than its crystalline counterparts,



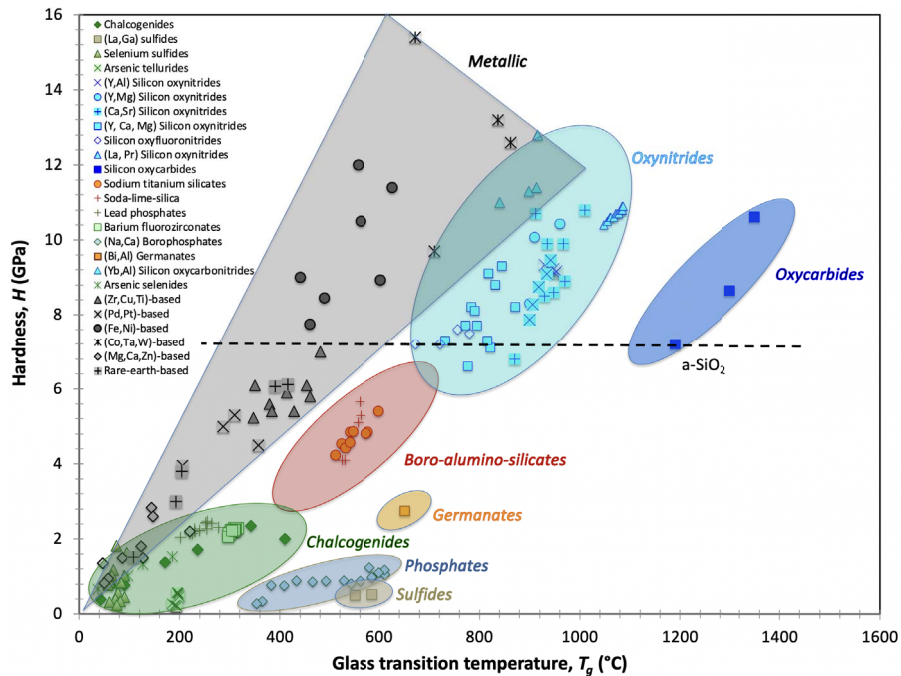


**Figure 4.** The hardness of glass (mostly measured by means of the Vickers indentation test) as a function of the glass transition temperature. Reprinted and adapted from Ref. [12].

quartz ( $H = 10\text{--}12$  GPa), coesite ( $H \approx 10$  GPa) or than its high-density variant, the stishovite ( $H \approx 33$  GPa) [17, 18] (Figure 5). With an increase in the packing density, the bond strength becomes more important than the packing density itself, and hardness is more and more controlled by the resistance the glass offer to the shear flow. This is why MGs can be stiffer than—and as hard as—oxide glasses, despite much weaker interatomic bonding, thanks to a remarkable atomic packing density.

In the case of crystalline materials, and especially metals, the residual indentation print can be attributed to the movement of dislocation and is chiefly correlated to the shear modulus (per the Peierls expression for the lattice friction force), and to a lesser extent to some diffusion processes (especially at elevated temperature) when the transport of matter plays a role in the permanent deformation, as in the cases of dislocation climb or diffusion creep for example. Therefore, hardness values are typically below 3 GPa for metals, and  $H$  is proportional to the macroscopic flow stress and to the shear modulus:  $H \approx 0.01\mu$  (Figure 4). MGs, which deform by localized shear-transformation-zone processes [19], are mostly hard ( $H$  ranges between 2 and 18 GPa) and exhibit a much larger slope,  $H \approx 0.145\mu$ , but smaller than the one for silicate glasses,  $H \approx 0.2\mu$ . As a consequence, although MGs are mostly much stiffer than silicate glasses, they are only slightly harder. The differences observed between these classes of materials derive from the fundamental changes in the deformation mechanism and is discussed below.

The possible and eventually concomitant mechanisms resulting in a permanent imprint at the surface of glass in ambient conditions include (i) densification; (ii) isochoric shear flow; and (iii) damage-based processes (microcracking) [20]. The stress in the contact area, which decreases toward the hardness value upon loading (as the contact area grows), is obviously much larger than the stress that glasses can withstand during “ordinary” mechanical testing (such



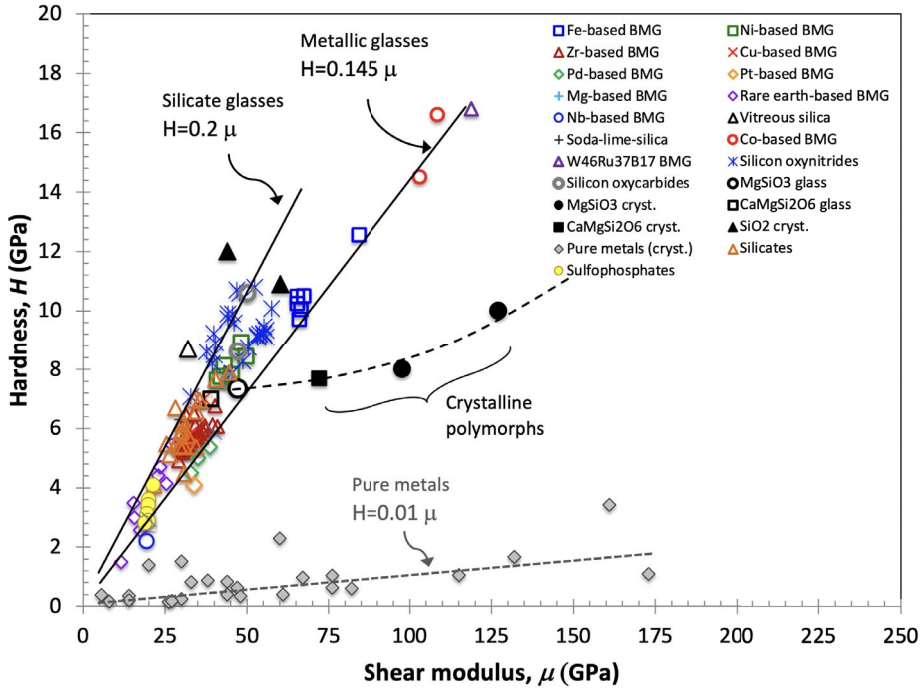


**Figure 5.** The hardness of glass as a function of the shear modulus. Data on crystallized polymorphs and metamorphic minerals were taken from Refs. [17, 18]. Other data are from Refs. [4, 6, 12].

as bending or compression tests) or in service conditions, and are sufficient to generate some densification in the process zone beneath the imprint. Densification at indentation sites was deduced from changes in the refractive index as measured by optical interferometry [21, 22], as well as by Raman spectroscopy [23, 24], and was recognized to be a general property of inorganic non-metallic glasses. Densification, which is a displacive transformation, shows up through a persistent change of the atomic network structure in the region that extends up to several times the indentation size beneath the surface, and involves a collapse of matter into a relatively-more close packed structure. The extent to which a glass can densify during indentation depends on its atomic packing density. The smaller  $C_g$  is, and the larger the magnitude of the volume shrinkage becomes. In the case of amorphous silica (a-SiO<sub>2</sub>), densification accounts for 80% of the indentation volume, whereas for a Zr-based MGs, which has a random close packed structure, it contributes to less than 10% of the deformed volume [11, 25]. A striking feature of the densification mechanism is that it is promoted and eventually triggered by shear [26]. The temptation is thus great to use an additive relationship for the shear and the pressure contribution, as was suggested by independent research teams [27, 28], who proposed a yield function  $f(\bar{\sigma})$  that resembles the Mohr–Coulomb law used in soil mechanics (including granular media) where the local shear is represented by  $\tau_{\text{Max}}$ , or the Drucker–Prager criterion used in structure mechanics where an equivalent shear stress is considered, but in which both shear and pressure work in favour of yielding (unlike in soil mechanics)

$$f(\bar{\sigma}) = -\sigma_h + \zeta \tau_e - \sigma_o \quad (4)$$

where  $\bar{\sigma}$  is the stress tensor,  $\sigma_h$  is the hydrostatic stress (mostly  $<0$  beneath the contact area),  $\tau_e$  is an equivalent shear stress (for instance  $\tau_e = \sqrt{3} \cdot \bar{s}/2$  where  $\bar{s}$  is the deviatoric stress),  $\sigma_o$  is

the critical yield stress (pressure) in absolute value, and  $\zeta$  determines the sensitivity to the shear component.

However, whereas the former expression supposes that shear would itself be able to induce irreversible yield in the absence of any pressure, provided  $\zeta\tau_e = \sigma_o$ , there is no evidence that densification, which accounts for over 80% of the indentation print in a-SiO<sub>2</sub>, can occur solely in shear. An alternate proposition in line with the schematic drawing proposed by Mackenzie [26] is that shear plays the role of a trigger of an instability process (kinematics), involving local shape changes of structural units of the glass network, and resulting in a global volume contraction further driven by pressure. This mechanism could resemble the one by which a folding chair is folded hence reducing the space it occupies. The “folding chair” yield criterion could be written

$$f(\bar{\sigma}) = -[1 + \zeta'(\tau_e)]\sigma_h - \sigma_o \quad (5)$$

where  $\zeta'(\tau_e) \geq 0$  and  $\zeta'(0) = 0$ .

A simple form for the shear function could be  $\zeta'(\tau_e) = |\tau_e|/\tau_n$  where  $\tau_n$  is a normalizing constant. Further investigations in this area should account for some key and seemingly unique features of the densification of amorphous silica such as (i) the astonishing shear yield strength dependence on pressure [29], which is intimately linked to structural rearrangements (in particular the increase in the Si coordination number) occurring at the atomic scale, and (ii) the strong non-linear elastic behaviour that shows up in glass in the stress range of concern, and (iii) the dramatic change in the elastic properties occurring as densification proceeds.

Beside densification, the other major contribution to the formation of an imprint is the isochoric and shear-driven flow of matter. The shear deformation processes, which are reconstructive by nature, may greatly differ depending on the material. Shear-thinning viscous flow, where the non-linear rheological behavior stems from the high pressure that builds at indentation site, can be invoked for non-metallic glasses. In the case of MGs, the fundamental unit processes of deformation occur via the collective shuffling of clusters of atoms to accommodate the applied shear strain. These are termed “shear transformation zones” (STZs), and result in an inhomogeneous plastic flow into narrow shear bands with typical thickness of  $\sim 10$  nm [19, 30]. These shear bands, after propagating through a characteristic distance, become shear cracks. The absence of dislocations in MGs, however, makes them considerably harder than their crystalline counterparts.

Whereas elastic moduli, and at the first place  $K$ , can be seen as bulk material properties, reflecting the energy content per unit volume in the material, or in other words the arrangement of bonds in space, hardness accounts for some fine heterogeneous details of the atomic organization, such as the presence of easy shear paths (slip planes for crystals, weak channels in glass).

#### 4. Strength, fracture surface energy and fracture toughness

The intrinsic strength of silica and silicate glasses is of the order of 14–20 GPa in vacuum, as shown both experimentally in tension [31] and by MD simulation [32]. However, the strength of a-SiO<sub>2</sub> decreases down to 6–7 GPa in moisture environment [31] and, indeed, some more recent studies dealing with the behavior of  $\mu\text{m}$  size micropillars suggested a yield stress (plastic flow) in compression in air of about 7 GPa [33]. The fracture surface energy ( $\gamma$ ) of a-SiO<sub>2</sub>, as obtained in vacuum using the double-cantilever-cleavage technique [34] is equal to  $3.62 \text{ J}\cdot\text{m}^{-2}$ . Taking a value of 70 GPa for Young’s modulus ( $E$ ) and 20 GPa for  $\sigma_d$  further results in a critical distance  $r_0$  equal to 1.27 nm in the Orowan–Gilman equation for the theoretical cohesive strength:

$$\sigma_d = \sqrt{\frac{2\gamma E}{r_0}}. \quad (6)$$

This value is much larger (by about one order of magnitude) than any near-neighbor interatomic distances in glasses. For example, the Si–O distance in a-SiO<sub>2</sub> is close to 1.62 Å. Glasses are characterized by some medium range ordering occurring at a mesoscale, with a length scale in-between the interatomic distance and say a few nanometers, and involving structural units such as chains (chalcogenides), clusters (MGs), and rings (silicates, borates, etc.). For example, rings consisting of SiO<sub>4</sub> tetrahedra connected through Si–O–Si bridges of different sizes are found in a-SiO<sub>2</sub> and silica-rich glasses. Although the average ring size is at about 6 Å and corresponds to 6–8 members rings, some larger rings, with 10–12 members are observed, with a size that approaches the critical  $r_0$  value, and this is presumably the weakest link of the atomic network where fracture is initiated. The value for  $r_0$  being much larger than any distance at the short-order arrangement scale, it is hypothesized that the critical length it is not much affected by compositional changes within a specific chemical system.

Ductility can be assessed in different ways, such as by means of the measurement of the tensile strain at fracture or using fracture toughness measurements. In the latter case, the measured fracture toughness value ( $K_{Ic}$  in opening mode) mostly accounts for the occurrence of dissipation mechanisms at the vicinity of the crack front, such as confined plasticity and viscoplasticity. As a matter of fact, the obtained  $K_{Ic}$  values are much larger than the one that would be predicted from the Irwin–Griffith similarity principal:

$$K_{Ic} = \sqrt{2E'\gamma} \quad (7)$$

where  $E' = E/(1 - \nu^2)$  and  $E' = E$  respectively in plane strain and in plane stress situations.

Consequently,  $K_{Ic}$  can no longer be considered as an intrinsic property of the material as it strongly depends on the loading-rate, on temperature and also on the sample size in cases where the confined deformation zone extends to a significant fraction of the specimen thickness. In this regard, inorganic and non-metallic glasses offer a unique opportunity to measure the intrinsic toughness, that is a parameter directly related to the energy required to create the fracture surface through a bond disruption process, provided the crack is atomically sharp. In order to fulfil this requirement, a few self-consistent methods were successfully applied to glass samples from different chemical systems but metallic ones, namely the Controlled Surface Flaw technique (CSF), the Chevron-Notched beam technique (CN), and the Single Edge Pre-cracked Beam technique (SEPB) (see Ref. [35] for details). The experimental results are plotted as a function of hardness in Figure 6. The general trend is that the hardest materials are also the most brittle. Nevertheless, the fine details within a class of materials might be different, and as a matter of fact, the toughest glasses among non-metallic inorganic systems, namely the silicon oxynitride glasses, are also the hardest ones!

In addition to the experimental investigations, a relatively simple approach to predict  $\gamma$  and  $K_{Ic}$  in a quantitative manner consists in assuming that a propagating crack extends following a path disrupting the weakest links of the energy landscape, and to estimate the surface energy from the bond strength and the bond concentration along this fracture surface [36]. The intrinsic (or theoretical) fracture surface energy is obtained from the surface density of representative structural units and from the relevant bond strength. This approach was successfully applied to relatively complex glass systems replacing the cleavage plane by a plane of arbitrary orientation (random) and taking the number of disrupted bonds from the stoichiometric formula (gram-atom) and assuming that a crack preferentially cuts the weakest links of the network. Let  $x_i$  be the stoichiometric fraction of the species involved in the  $i$ th bonding energy  $U_{oi}$  (in J·mol<sup>-1</sup>), between the  $i$ th cation ( $A_i$ ) and a first neighbor oxygen anion in the case of an oxide glass, and let  $n_i$  be the number of such bonds supposed to be broken as the crack front propagates to the

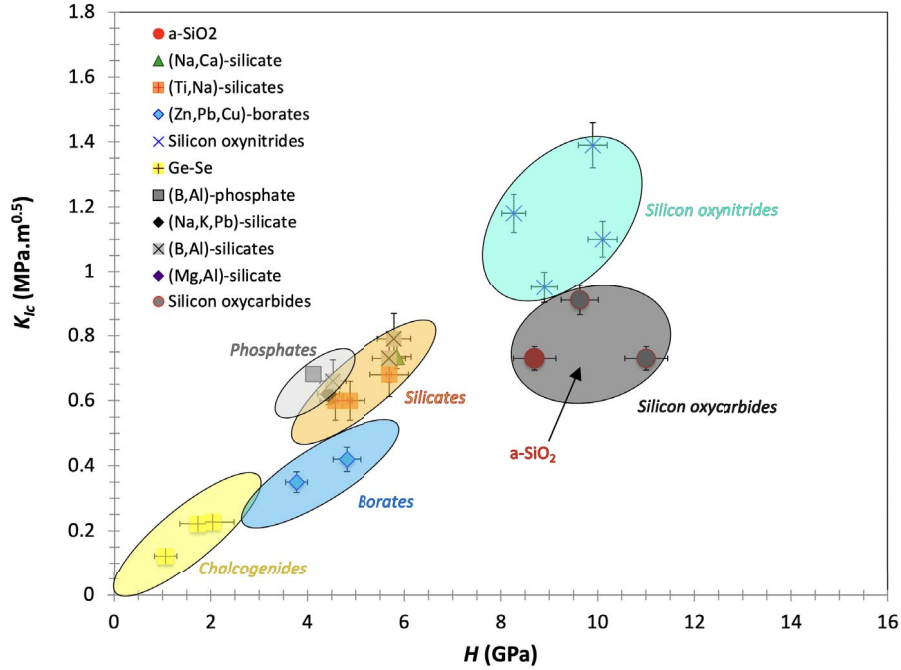


**Figure 6.** The fracture toughness (intrinsic) of glasses from different chemical systems as a function of hardness. Data were extracted from Refs. [36, 37].

next unit, then  $\gamma$  is expressed as:

$$\gamma = \frac{1}{2} \left( \frac{\rho}{M_0} \right)^{2/3} \mathcal{N}^{-1/3} \sum_i x_i n_i U_{oi} \quad (8)$$

where the 1/2 pre-factor on the right-hand side member accounts for the fact that the bond disruption process leads to the formation of two complementary surfaces.

An equivalent expression to (8) is obtained with  $C_g$ :

$$\gamma = \frac{1}{2} \left( \sum_i \frac{4}{3} \pi x_i r_i^3 \right)^{-2/3} \mathcal{N}^{-1} C_g^{2/3} \langle U_0 \rangle \quad (9)$$

where  $\langle U_0 \rangle = \sum_i x_i n_i U_{oi}$  is the mean energy content in a gram-atom of glass.

Some theoretical and experimental data were extracted from Refs. [36–43] and are summarized in Table 1. The agreement between the theoretical (last two columns) and experimental values of  $\gamma$  for glasses from various chemical systems corroborate the assumption that the crack front opening displacement is within the interatomic distance, and fracture is purely elastic.

As far as non-metallic inorganic glasses are concerned,  $K_{Ic}$  and  $\gamma$  range typically from 0.1 to 1.5  $\text{MPa}\cdot\sqrt{\text{m}}$  and from 0.5 to 8  $\text{J}\cdot\text{m}^{-2}$  respectively. The most brittle glasses are found in the chalcogenide and lead-borate systems, which turn out to exhibit at the same time a relatively large atomic packing density and a relatively small interatomic bond strength. In contrast, silicon oxynitride and oxycarbide glass forming systems provide the toughest glasses. The situation is nevertheless different in these latter systems. In the case of silicon oxynitride glasses, the large  $K_{Ic}$  values are attributed to the efficient packing of strongly bonded atoms (these glasses are also the stiffest), whereas in the case of silicon oxycarbide, the resistance toward crack initiation is supposed to derive from the important 3D cross-linking of a network consisting of strong bonds, and on possible crack tip shielding phenomena as the crack meets the nanoscale cavities

**Table 1.**  $K_{Ic}$  and  $\gamma$  of glasses from different chemical systems (from Refs [36, 37])

Glass	$E$ (GPa)	$\nu$	$K_{Ic}$ (MPa·m <sup>0.5</sup> )	Method	$\gamma$ (8) (J·m <sup>-2</sup> )	$K_{Ic}$ (7) (MPa·m <sup>0.5</sup> )
a-SiO <sub>2</sub>	70	0.15	0.73	DCC (in vac.) [38]	3.62	0.718
Si <sub>0.25</sub> Na <sub>0.92</sub> Ca <sub>0.035</sub> Mg <sub>0.021</sub> O <sub>0.602</sub>	72	0.224	0.7	3.55 [36]		0.734
Ti <sub>0.013</sub> Si <sub>0.287</sub> Na <sub>0.067</sub> O <sub>0.633</sub>	65.3	0.215	0.68	SEPB [39]	3.57	0.70
Ti <sub>0.013</sub> Si <sub>0.270</sub> Na <sub>0.1</sub> O <sub>0.617</sub>	66.1	0.201	0.6	SEPB [39]	3.55	0.699
Ti <sub>0.013</sub> Si <sub>0.253</sub> Na <sub>0.133</sub> O <sub>0.6</sub>	63.9	0.232	0.6	SEPB [39]	3.46	0.679
Ti <sub>0.037</sub> Ba <sub>0.111</sub> Si <sub>0.222</sub> O <sub>0.63</sub>	74.9	0.276	0.47	SEPB [36]	0.86	0.374
Si <sub>0.196</sub> Na <sub>0.008</sub> K <sub>0.005</sub> Pb <sub>0.196</sub> O <sub>0.595</sub>	55	0.248	0.62	CN [40]	2.83	0.576
Pb <sub>1/7</sub> B <sub>2/7</sub> O <sub>4/7</sub>	57.5	0.289	0.35	SEPB [36]	0.88	0.332
Pb <sub>0.114</sub> B <sub>0.286</sub> Cu <sub>0.029</sub> O <sub>0.571</sub>	67.4	0.298	0.42	SEPB [36]	0.86	0.358
Zn <sub>1/7</sub> B <sub>2/7</sub> O <sub>4/7</sub>	80.9	0.33	0.4	SEPB [36]	0.62	0.336
Si <sub>0.215</sub> K <sub>0.031</sub> B <sub>0.123</sub> O <sub>0.631</sub>	64	0.233	0.73	SEPB [41]	4.09	0.744
Si <sub>0.226</sub> Al <sub>0.065</sub> B <sub>0.065</sub> O <sub>0.645</sub>	70	0.208	0.79	SEPB [41]	4.03	0.767
Si <sub>0.235</sub> B <sub>0.039</sub> Pb <sub>0.098</sub> O <sub>0.627</sub>	63	0.261	0.66	SEPB [41]	3.67	0.704
Si <sub>0.245</sub> Na <sub>0.024</sub> Al <sub>0.012</sub> B <sub>0.079</sub> O <sub>0.639</sub>	63.7	0.2	0.68	CN [42]	3.88	0.718
P <sub>0.216</sub> Al <sub>0.038</sub> K <sub>0.056</sub> Ba <sub>0.023</sub> Nd <sub>0.008</sub> O <sub>0.659</sub>	50	0.256	0.48	CN [40]	2.55	0.522
Y <sub>4.70</sub> Mg <sub>6.56</sub> Si <sub>16.78</sub> Al <sub>11.67</sub> O <sub>51.5</sub> N <sub>8.75</sub>	134	0.28	1.18	CN [43]	3.73	1.04
Ge <sub>0.15</sub> Se <sub>0.85</sub>	13.8	0.295	0.122	CN [36]	2.29	0.26
Ge <sub>0.25</sub> Se <sub>0.75</sub>	16.1	0.281	0.215	CN [36]	1.77	0.25
Ge <sub>0.3</sub> Se <sub>0.7</sub>	17.9	0.264	0.210	CN [36]	1.55	0.24
SiO <sub>0.141</sub> C <sub>0.3</sub>	96.7	0.18	0.73	SEPB [37]	nd	nd
SiO <sub>1.82</sub> C <sub>0.42</sub> Zr <sub>0.1</sub>	85.4	0.21	0.91	SEPB [37]	nd	nd

The theoretical value for  $K_{Ic}$  is derived from  $\gamma$ ,  $E$  and  $\nu$  using the plane strain assumption. Experimental errors are typically of  $\pm 1$  GPa for the elastic moduli and  $\pm 0.05$  MPa· $\sqrt{m}$  for fracture toughness as measured by the SEPB or CN methods. DCC stands for Double Cantilever Cleavage (also known as Double Cantilever Beam) specimen. “nd” stands for “non-determined”.

where the free volume concentrates. It is noteworthy that the most brittle glasses, namely the chalcogenides, are also the softest!

## 5. Conclusion

Interatomic bonds are quite similar in a glass and its crystallized polymorphs. Nevertheless, the atomic bonding arrangement in space is different. In particular, the presence of free volume makes the volume density of bonds, and thus the density of energy, smaller in glasses. Therefore, elastic moduli, which are given in J·m<sup>3</sup> (Pa), are usually smaller. Consequently, the bulk modulus of different polymorphs depends nearly linearly on the atomic packing density. The free volume content, or the atomic packing density has a tremendous influence on the elastic moduli of glasses, and predominates over the bond strength in many cases. This is why silicon oxynitride glasses are much stiffer than their parent oxide glasses or why sodium alumino-silicate glasses are stiffer than sodium alumino-borate glasses despite the fact that the Si–N bond is weaker than the Si–O one and the B–O bond strength is larger than the Si–O one.

However, as far as mechanical properties are concerned, it is important to distinguish phenomena occurring at the global scale such as volumetric change, and those occurring at some mesoscopic scale that are more heterogeneous in nature, such as shear-induced processes and fracture. These latter phenomena are mediated by the fine heterogeneous details of the atomic network (sliding and cleavage planes in crystals and easy shear paths in glass).

Hardness is intimately linked to a combination of contributing deformation mechanisms, including densification and shear processes. Therefore, it is a composite property involving both the global and the mesoscale at which shear localization occurs. The ease for dislocation glide in pure metals makes them relatively soft in comparison to metallic glasses, which are typically 15 times harder for a given shear modulus. Ionocovalent crystals are advantaged by a more efficient atomic packing than the glass with the same composition (when such a material exists) and are mostly (slightly) harder than their amorphous counterparts.

The intrinsic fracture surface energy ( $\gamma$ ) is intimately linked to the crack path. For “simple” mono-constituent glass such as a-SiO<sub>2</sub>, the experimental value for  $\gamma$  is in agreement with the prediction based on a random planar fracture path through the glass. In the case of multicomponent systems, it is necessary to account for the weakest links of the atomic network. Fracture toughness, as measured from a self-consistent method involving an atomically sharp crack ranges from 0.1 to 1.5 MPa·√m ( $\gamma$  is between 0.5 and 8 J·m<sup>-2</sup>), silicon oxynitride and oxycarbide glasses being the toughest among non-metallic inorganic glasses. Interestingly, the toughest glasses are also the hardest ones.

## Conflicts of interest

The author has no conflict of interest to declare.

## References

- [1] S. F. Pugh, “Relations between the elastic moduli and the plastic properties of polycrystalline pure metals”, *Philos. Mag. Ser.* **45** (1954), no. 367, p. 823-843.
- [2] D. Tabor, *The Hardness of Metals*, Clarendon Press, Oxford, 1951.
- [3] A. Makishima, J. D. Mackenzie, “Direct calculation of Young’s modulus of glass”, *J. Non-Cryst. Sol.* **12** (1973), p. 35-45.
- [4] T. Rouxel, “Elastic properties and short-to-medium range order in glasses”, *J. Am. Ceram. Soc.* **90** (2007), no. 10, p. 3019-3039.
- [5] D. R. Lide (ed.), *Handbook of Chemistry and Physics*, 86 ed., Taylor & Francis, 2005–2006.
- [6] T. Rouxel, Y. Yokoyama, “Elastic properties and atomic bonding character in metallic glasses”, *J. Appl. Phys.* **118** (2015), article no. 044901.
- [7] F. R. de Boer *et al.*, in *Cohesion in Metals—Transition Metal Alloys* (F. R. de Boer, D. G. Pettifor, eds.), Elsevier Science, 1989.
- [8] G. N. Greaves, A. L. Greer, R. S. Lakes, T. Rouxel, “Poisson’s ratio and modern materials”, *Nat. Mater.* **10** (2011), p. 823-837.
- [9] R. Limbach, A. Winterstein-Beckmann, J. Dellith, D. Möncke, L. Wondraczek, “Plasticity, crack initiation and defect resistance in alkali-borosilicate glasses: from normal to anomalous behavior”, *J. Non-Cryst. Sol.* **417–418** (2015), p. 15-27.
- [10] S. Striepe, N. Da, J. Deubener, L. Wondraczek, “Micromechanical properties of (Na, Zn)-sulfophosphate glasses”, *J. Non-Cryst. Sol.* **358** (2012), p. 1032-1037.
- [11] T. Rouxel, H. Ji, T. Hammouda, A. Moréac, “Poisson’s ratio and the densification of glass under high pressure”, *Phys. Rev. Lett.* **100** (2008), article no. 225501.
- [12] T. Rouxel, J. I. Jang, U. Ramamurty, “Indentation of glasses”, *Prog. Mat. Sci.* **121** (2021), article no. 100834.
- [13] H. Li, C. Bradt, “The indentation load/size effect and the measurement of the hardness of vitreous silica”, *J. Non-Cryst. Sol.* **146** (1992), p. 197-212.
- [14] G. D. Quinn, P. Green, K. Xu, “Cracking and the indentation size effect for Knoop hardness of glasses”, *J. Am. Ceram. Soc.* **86** (2003), p. 441-448.
- [15] P. Sellappan, T. Rouxel, F. Celarié, E. Becker, P. Houzot, R. Conrard, “Composition dependence of indentation deformation and indentation cracking in glass”, *Acta Mater.* **61** (2013), p. 5949-5965.
- [16] R. Limbach, A. Winterstein-Beckmann, J. Dellith, D. Möncke, L. Wondraczek, “Plasticity, crack initiation and defect resistance in alkali-borosilicate glasses: from normal to anomalous behavior”, *J. Non-Cryst. Sol.* **417–418** (2015), p. 15-27.
- [17] E. Kulik, N. Nishiyama, Y. Higo, N. A. Gaida, T. Katsura, “Hardness of polycrystalline SiO<sub>2</sub> coesite”, *J. Am. Ceram. Soc.* **102** (2019), p. 2251-2256.

- [18] D. L. Whitney, M. Broz, R. Cook, "Hardness, toughness, and modulus of some common metamorphic minerals", *Am. Mineral.* **92** (2007), p. 281-288.
- [19] W. H. Wang, C. Dong, C. H. Shek, "Bulk metallic glasses", *Mater. Sci. Eng.* **R44** (2004), p. 45-89.
- [20] T. Rouxel, H. Ji, J. P. Guin, F. Augereau, B. Rufflé, "Indentation deformation mechanism in glass: densification versus shear flow", *J. Appl. Phys.* **107** (2010), article no. 094903.
- [21] F. M. Ernsberger, "Role of densification in deformation of glasses under point loading", *J. Am. Ceram. Soc.* **51** (1968), p. 545-547.
- [22] K. W. Peter, "Densification and flow phenomena of glass in indentation experiments", *J. Non-Cryst. Sol.* **5** (1970), p. 103-115.
- [23] A. Perriot, D. Vandembroucq, E. Barthel, V. Martinez, L. Grosvalet, C. Martinet, B. Champagnon, "Raman microscopic characterization of amorphous silica plastic behavior", *J. Am. Ceram. Soc.* **89** (2006), p. 596-601.
- [24] H. Ji, *Mécanique et physique de l'indentation du verre*, PhD Thesis, University of Rennes 1, France, 2007.
- [25] S. Yoshida, J. C. Sangleboeuf, T. Rouxel, "Quantitative evaluation of indentation-induced densification in glass", *J. Mater. Res.* **20** (2005), p. 3404-3412.
- [26] J. D. Mackenzie, R. P. Laforce, "High-pressure densification of glass and the effects of shear", *Nature* **197** (1963), p. 480-481.
- [27] J. C. Lambropoulos, S. Xu, T. Fang, "Constitutive law for the densification of fused silica, with applications in polishing and microgrinding", *J. Am. Ceram. Soc.* **79** (1996), p. 1441-1452.
- [28] G. Kermouche, E. Barthel, D. Vandembroucq, Ph.. Dubujet, "Mechanical modelling of indentation-induced densification in amorphous silica", *Acta Mater.* **56** (2008), p. 3222-3228.
- [29] C. Meade, R. Jeanloz, "Effect of a coordination change on the strength of amorphous SiO<sub>2</sub>", *Science* **241** (1988), no. 4869, p. 1072-1074.
- [30] M. D. Marsh, "Plastic flow and fracture of glass", *Proc. R. Soc. Lond. A* **282** (1964), no. 1388, p. 33-43.
- [31] B. A. Proctor, I. Whitney, J. W. Johnson, "The strength of fused silica", *Proc. R. Soc. Lond. A* **297** (1967), p. 534-557.
- [32] F. Yuan, L. Huang, "Brittle to ductile transition in densified silica glass", *Sci. Rep.* **4** (2014), article no. 5035.
- [33] R. Lacroix, G. Kermouche, G. Teisseire, E. Barthel, "Plastic deformation and residual stresses in amorphous silica pillars under uniaxial loading", *Acta Mater.* **60** (2012), no. 15, p. 5555-5566.
- [34] S. M. Wiederhorn, "Fracture surface energy of glass", *J. Am. Ceram. Soc.* **52** (1969), no. 2, p. 99-105.
- [35] T. To, F. Célarié, C. Roux-Langlois, A. Bazin, Y. Gueguen, H. Orain, M. Le Fur, V. Burgaud, T. Rouxel, "Fracture toughness, fracture energy and slow crack growth of glass as investigated by the Single-Edge Pre-cracked Beam (SEPB) and Chevron-Notched Beam (CNB) methods", *Acta Mater.* **146** (2018), p. 1-11.
- [36] T. Rouxel, "Fracture surface energy and toughness of inorganic glasses", *Scr. Mater.* **137** (2017), p. 109-113.
- [37] T. To, C. Stabler, E. Ionescu, R. Riedel, F. Célarié, T. Rouxel, "Elastic properties and fracture toughness of SiOC-based glass-ceramic nanocomposites", *J. Am. Ceram. Soc.* **103** (2020), p. 491-499.
- [38] S. M. Wiederhorn, H. Johnson, A. M. Diness, A. H. Heuer, "Fracture of glass in vacuum", *J. Am. Ceram. Soc.* **57** (1974), no. 8, p. 336-341.
- [39] G. Scannell, D. Laillé, F. Célarié, L. Huang, T. Rouxel, "Interaction between deformation and crack initiation under Vickers indentation in Na<sub>2</sub>O-TiO<sub>2</sub>-SiO<sub>2</sub> glasses", *Front. Mater.* **4** (2017), article no. 6.
- [40] P. Vullo, M. J. Davis, "Comparative study of micro-indentation and Chevron notch fracture toughness measurements of silicate and phosphate glasses", *J. Non-Cryst. Sol.* **349** (2004), p. 180-184.
- [41] Y. Kato, H. Yamazaki, S. Yoshida, J. Matsuoka, "Effect of densification on crack initiation under Vickers indentation test", *J. Non-Cryst. Sol.* **356** (2010), p. 1768-1773.
- [42] K. P. R. Reddy, E. H. Fontana, J. Helfinstine, "Fracture toughness measurement of glass and ceramic materials using Chevron-notched specimens", *J. Am. Ceram. Soc.* **71** (1988), p. C-310-C-313.
- [43] T. Rouxel, Y. Laurent, "Fracture characteristics of SiC particle reinforced oxynitride glass using chevron-notch three-point bend specimens", *Int. J. Fract.* **91** (1999), p. 83-101.